# Development of a bio-inspired transformable robotic fin



2016 Bioinspir. Biomim. 11 056010

(http://iopscience.iop.org/1748-3190/11/5/056010)

IOP Publishing Bioinspir. Biomim. 11 (2016) 056010 doi:10.1088/1748-3190/11/5/056010

Bioinspiration & Biomimetics

CrossMark

RECEIVED
23 April 2016

REVISED
16 July 2016

ACCEPTED FOR PUBLICATION
25 July 2016

PUBLISHED
31 August 2016

PAPER

# Development of a bio-inspired transformable robotic fin

**Yikun Yang[1], Yu Xia[1], Fenghua Qin[2], Min Xu[1], Weihua Li[3] and Shiwu Zhang[1,4]**

[1] Department of Precision Machinery and Precision Instrumentation, University of Science and Technology of China, Hefei, Anhui 230027, People's Republic of China
[2] Department of Modern Mechanics, University of Science and Technology of China, Hefei, Anhui 230027, People's Republic of China
[3] School of Mechanical, Materials and Mechatronic Engineering, University of Wollongong, Wollongong, NSW 2522, Australia
[4] Author to whom any correspondence should be addressed.

**E-mail:** ykyang@mail.ustc.edu.cn, xy1993@mail.ustc.edu.cn, qfh@ustc.edu.cn, xumin@ustc.edu.cn, weihuali@uow.edu.cn and swzhang@ustc.edu.cn

**Keywords:** transformable robotic fin, thrust force, efficiency, controlling mode

## Abstract

Fish swim by oscillating their pectoral fins forwards and backwards in a cyclic motion such that their geometric parameters and aspect ratios change according to how fast or slow a fish wants to swim; these complex motions result in a complicated hydrodynamic response. This paper focuses on the dynamic change in the shape of a fin to improve the underwater propulsion of bio-inspired mechanism. To do this, a novel transformable robotic fin has been developed to investigate how this change in shape affects the hydrodynamic forces acting on the fin. This robotic fin has a multi-link frame and a flexible surface skin where changes in shape are activated by a purpose designed multi-link mechanism driven by a transformation motor. A drag platform has been designed to study the performance of this variable robotic fin. Numerous experiments were carried out to determine how various controlling modes affect the thrust capability of this fin. The kinematic parameters associated with this robotic fin include the oscillating frequency and amplitude, and the drag velocity. The fin has four modes to control the cyclic motion; these were also investigated in combination with the variable kinematic parameters. The results will help us understand the locomotion performance of this transformable robotic fin. Note that different controlling modes influence the propulsive performance of this robotic fin, which means its propulsive performance can be optimized in a changing environment by adapting its shape. This study facilitates the development of bio-inspired unmanned underwater vehicles with a very high swimming performance.

## 1. Introduction

Fish are an intrinsic part of the marine kingdom, so it is no surprise that their graceful swimming has attracted the attention of researchers while providing a vast amount of inspiration and imagination for designing and developing robotic fish [1–4]. Not unnaturally, the wide variety of fish and their various shaped fins were created to perfectly fit their marine environment. This wide variety of fin forms was designed for different modes of underwater propulsion. For instance, the caudal fins act as a dominant propeller with the pectoral fins, the dorsal fins and other fins assist in the body and caudal fin modes, the pectoral fin is the main propeller for the median and/or paired fin modes, while the dorsal fin and anal fin may be used to assist body position and stability in motion [5, 6]. Due to their prominent and multiple roles in propulsion and maneuvering, many studies have been carried out on fins, including their physiology, morphology, and kinematics, in order to adapt their structure and propulsive performance [7–12], to robotic fins [13–17].

Fish fins undergo large changes in shape during swimming. Lauder *et al* studied the flexible pectoral fin and caudal fin of bluegill sunfish during steady forward swimming and maneuvering motions [18–20], and found that fins exhibit complicated forms, whether in cruising or maneuvering mode that may be due to the active control of the fin ray or the passive alteration due to flexibility. Webb studied the form and function of fish while swimming and summed up the special roles played by caudal fins with different shapes. For example, a crescent fin is suitable for cruising; a trapezoid fin is better for accelerating; and a fan fin is good at maneuvering [21]. Their research inspired the development of a new technique for propulsion by mimicking biological fish.

Many bio-inspired and bio-mimetic robotic fishes have been developed to swim underwater; robotic fishes that mimic fishes from carangiform to ostraciiform are popular where faster swimming is required [22–28]. The propulsive force of these robotic fish is mainly generated by the caudal fin [29], so the shape of a robotic fin, particularly its aspect ratio, has an enormous effect on the propulsive force [30]. These facts have inspired researchers to develop robotic fish that can alter the shape of their fins to improve propulsion performance. The typical attempts include applying flexible foils on robotic fish [31–35], varying the surface area of the fin [36], and imitating structure of the bony fin [37–43], i.e. constructing the robotic fin with fin rays and membrane. The biomimetic structure enables the robotic fins to drive fin rays and perform a complex three-dimensional deformation during the oscillation to improve propulsion. However, in most situations, the shapes of robot fin, especially the aspect ratio of the fin, cannot be changed during swimming. In this paper, we report the design and implementation of a transformable robotic fin that can vary its aspect ratio smoothly and gradually during one cycle of propulsion. The robotic fin can fulfill three kinds of typical homocercal shapes, that is, fan, trapezoid, and crescent [21]. The detailed design and experiments carried out on this robotic fin are presented here. Developing this transformable fin shed light on the applications of an adaptive robotic fish in complex and changing environments.

The reminder of the paper is organized as follows: section 2 presents the design of the transformable fin that can synchronously oscillate and transform. The experimental platform is explained. Sections 3 and 4 present the experimental results of the fin with various kinematic parameters and controlling modes. Section 5 concludes the study.

## 2. Materials and methods

To improve the adaptation of a robotic fish to complex and continuously changing environments, transforming the robotic fin is an effective option for underwater propulsion.

### 2.1. Design of the transformable robotic fin

The structure of this robotic fin is shown in figure 1, and indicates how its shape can be changed by pushing or pulling the driving rod. It consists of a rigid multi-link frame and a flexible surface skin. The frame is made from carbon fiber, because it is light and very strong. The surface skin is made from a rubber membrane that can deform without rupturing. The fin changes shape as the non-elastic cable connected to the driving rod and transform motor is pulled; the elasticity in the surface skin also provide a restorative force as the robotic fin returns to its normal shape.

The design objective here is to gradually and smoothly transform a robotic fin from a crescent to a fan shape via the multi-linked mechanism shown in figure 1(a). As the driving rod moves along the keel rod, the multi-linked structure moves with the driving rod and changes the shape of the fin. Figure 1(b) shows this transformation process. The driving rod is driven by a non-elastic cable that moves smoothly along the keel rod so the fin can continuously transform from crescent to fan.

To calculate the change in the surface area and the aspect ratio of the robotic fin, we divided the fin into four parts, as shown in figure 2; $S_1$, $S_2$, $S_3$, and $S_4$. The area can be calculated with the following equations.

$$
\begin{aligned}
S_1 &= \frac{1}{2}(x+n)b;\ S_2 = \frac{1}{2}c \times \sqrt{b^2+(x+n)^2} \\
&\quad \times\ \sin\alpha_1, \\
S_3 &= c \times d \times \sin\alpha_2 \\
S_4 &= \frac{1}{2}e \times f \times\ \sin\alpha_3, \\
S &= (S_1+S_2+S_3+S_4) \times 2.
\end{aligned} \tag{1}
$$

And the aspect ratio of the transformable fin is defined as:

$$\lambda = l^2/S, \tag{2}$$

where $x$ denotes the distance the driving rod moves, $n$ denotes the distance from the fix block to the hinge point, $b$ denotes the half length of the driving rod, $c$, $e$ and $f$ represent the length of the links, respectively, $d$ denotes the span of the caudal fin, and $S$ represents the total area of the fin.

As figure 2 shows, as the shape changes from crescent to fan, the span of the fin does not change much, but the area is more than two times larger, and therefore the aspect ratio of the fin will be reduced twice.

### 2.2. Design of the experimental platform

To explore the propulsive performance of this transformable fin, theexperimental platform shown in figure 3 was developed. It consists of a synchronous belt, a towing platform, a driving module, and a two-dimensional force transducer. The driving module, towing platform, and two-dimensional force transducer (JLBS-v, Jnsensor, China) are connected to each other. A step motor (85BYGH, Shuangjie, China) is used to drive the towing platform at a speed of $V$ to simulate the drag velocity of the fin under water. To mimic a caudal fin oscillating under water, the driving module is combined with two motors to oscillate and change the shape of the robotic fin.

Figure 3(b) illustrates the whole experimental setup. To study the individual factors contributing to the performance of the fin, the experimental platform was developed without having the confounding

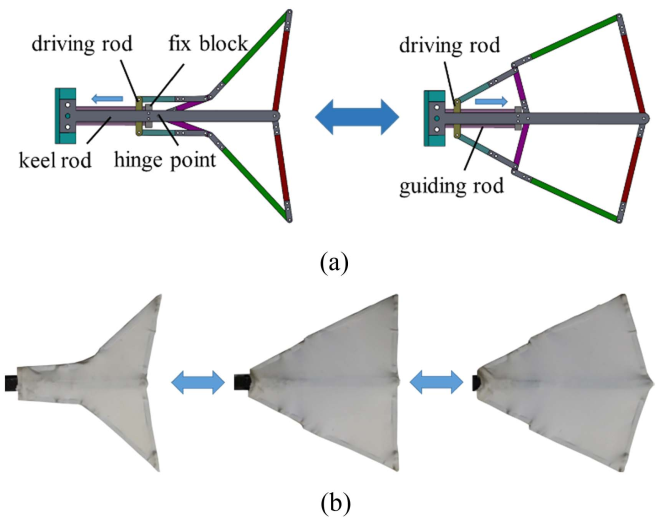


**Figure 1.** Transformable robotic fin which can gradually and smoothly change its shape. (a) structure of the transformable fin; (b) transformation process.

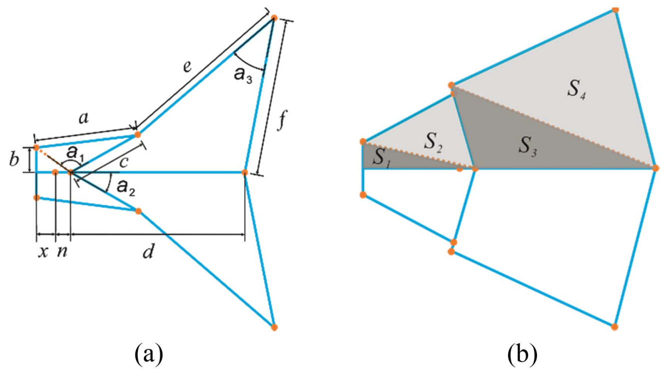


**Figure 2.** Calculation of surface area and aspect ratio of the transformable robotic fin. (a) The length of each rod; (b) the surface area division of the fin.

complexity of the whole fish [44]. A carbon fiber tube connects the driving module and transformable robotic fin, through which there is a non-elastic cable connected to the driving rod of the fin and the cable reel on the driving module. The experiments were carried out in a 2 m × 1 m × 0.8 m transparent tank. The fin sits in the middle of the water tank and even in the case of the maximum amplitude of 30°, the width of the transparent tank is still about five times as much as the moving distance of the distal end of the fin. Thus it can effectively reduce the interference from the walls and the surface of the water.

The driving module controls the oscillation and change in shape of the fin. The oscillating motor provides oscillating motion to the fin as it drives a gear set connected to the fin via the carbon fiber tube. By controlling the motor's reciprocating rotation we can achieve various oscillating frequencies and amplitudes of the robotic fin. To change the shape of the fin, the transformation motor drags the non-elastic cable around the cable reel. The cable bypasses the top and bottom pulley located in the carbon fiber tube and connects directly to the driving rod to switch from a rotating motion to a translational motion. As the cable moves, the driving rod moves along the keel rod and the robotic fin changes smoothly from crescent to fan. The rubber membrane provides a restoring force as the robotic fin returns to its normal shape. The moves in a reciprocating motion along the guiding rod, whereas the oscillating and shape changing motions of the robotic fin are independent of each other. Therefore, the robotic fin can be transformed as it oscillates.

### 2.3. Design of the experiment

The robotic fin undergoes an oscillating and shape changing motion, and an arbitrary combination of oscillation and shape changing, by which we can obtain a large number of controlling modes. However, this transformable fin has a twofold purpose, (a) to adopt a suitable shape when encountering a changing environment; (b) transform itself during an oscillating cycle to improve propulsion. This robot fin also has

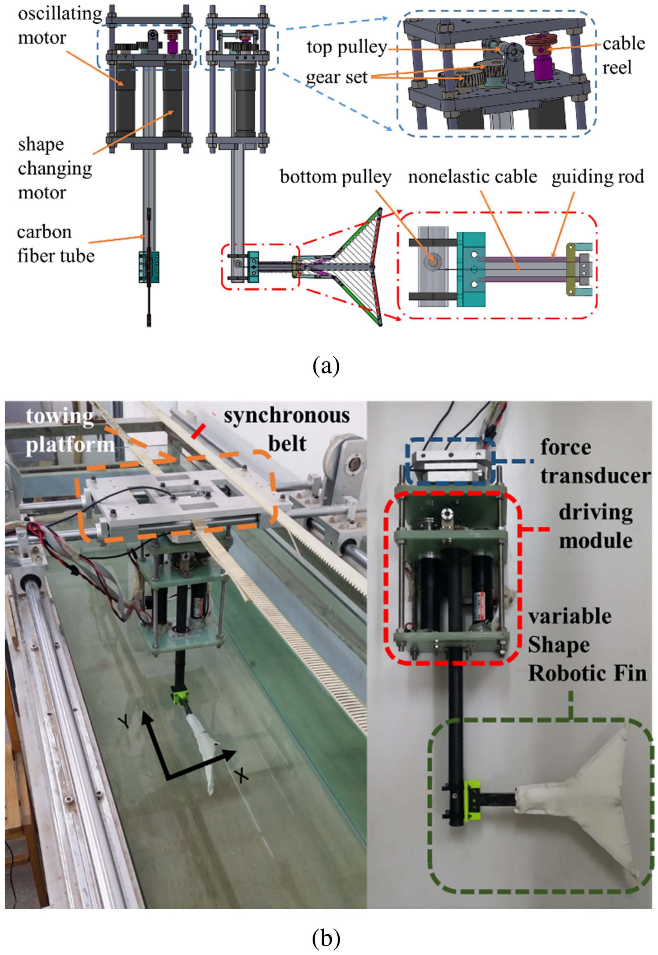


**Figure 3.** The experimental platform and the robotic fin. (a) Sketch of the driving module and the transformable fin. (b) Photography of the experimental platform.

two types of controlling modes, a steady mode and a transformation mode. For steady modes, the shape of the fin remains stable during oscillation, but in the transformation modes, the shape changes during one cycle of oscillation.

To consider biomimetic and practical issues, we selected two typical steady modes and two typical transformation modes to explore the propulsive performance of the robotic fin. The two steady modes include a minimum surface area mode and a maximum surface area mode, which we called the crescent mode and fan mode respectively. These two transformation modes include a crescent to fan mode, which means the fin transforms from crescent to fan while oscillating, and fan to crescent mode, which means the fin transforms from fan to crescent.

In the crescent to fan mode, the fin has a minimum area in two out-strokes and maximum area in two in-strokes. In fan to crescent mode, the fin has a maximum area in two out-strokes and a minimum area in two in-strokes. The relationship between the shape changing motion and oscillating motion of the four controlling modes is shown in figure 4.

In this study, three kinematic parameters and four controlling modes were combined and investigated. The parameters include the oscillating frequency ($f$), the oscillating amplitude ($\theta$), and the drag velocity ($L$). This means we can change the controlling modes according to different kinematic parameter combinations to increase adaptability in a changing environment and improve propulsive performance. The drag velocity simulates the swimming velocity of fish in varying environments. We selected five drag velocities to simulate the performance of the fin in downstream and counter-currents with different velocities. In this experiment, the drag velocity is imitated by the varying the movement of the towing platform from $-0.5\,L$ to $0.5\,L$, where $L$ represents the total length of the fin set at 170 mm.

To consider the capability of the robot fin and limitations of the force transducer, the parameters used in the experiment are listed below in table 1.

By combining the kinematic parameters and controlling modes, the experiment has 300 cases. To identify how various kinematic parameters and controlling modes would affect the propulsive performance of the fin, we selected typical data for analysis and

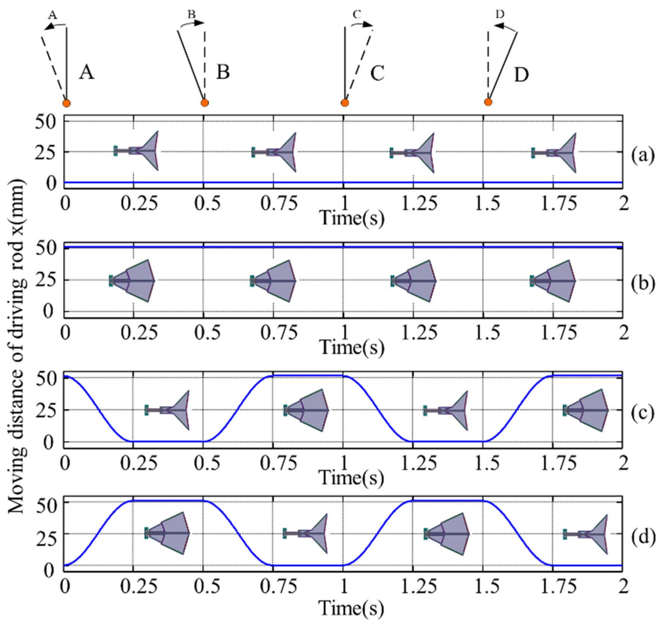


**Figure 4.** Four controlling modes. (a) Crescent mode; (b) fan mode; (c) crescent to fan mode; (d) fan to crescent mode. A and C stand for out-stoke stages respectively, while B and D stand for in-stroke stages respectively.

**Table 1.** Parameters used in experiment.

| Parameter | Specific value |
|---|---|
| Frequency, $f$(Hz) | 0.25 0.5 1 |
| Amplitude, $\theta$(degree) | 15 20 25 30 |
| Drag velocity, $v$ ($L$/s) | −0.5 −0.25 0 0.25 0.5 |

comparison. The control variable method was used to determine how each parameter influenced the robot fin [45].

### 2.4. Evaluation criterion

Two parameters were used to evaluate the propulsive performance of the transformable robotic fin, i.e., thrust force and propulsive efficiency, respectively. We defined the propulsive efficiency by the ratio of useful power consumption and total consumption of the robotic fin [24], as given below:

$$\eta = \frac{P_u}{P_w} = \frac{P_u}{P_a - P_m}. \tag{3}$$

In above equation, all calculations in the functions are for average power. The useful power consumption of the fin within a period is given in equation (4), and the total output power of the oscillating motor is defined as equation (5)

$$P_u = \bar{F} \cdot v, \tag{4}$$

$$P_a = \frac{\int_0^T M(t)\omega(t)\mathrm{d}t}{T}, \tag{5}$$

where the useful power consumption $P_u$ is defined as the average thrust force $\bar{F}$ multiples the drag velocity $v$. $P_a$ denotes the total output power of the oscillating motor, $M(t)$ denotes the output torque of the oscillating motor and $\omega(t)$ denotes the angular velocity of the oscillating motor. $P_a$ and the mechanical transmission power $P_m$ is obtained as the robotic fin undulates in water and air with the same locomotion parameters, and the total consumption of the fin model underwater $P_w$ is yielded by removing $P_m$ from the total power output:

$$P_w = P_a - P_m. \tag{6}$$

Note that two motors are needed to oscillate and change the shape of the fin during the transformation mode. In a steady state a motor is not needed to change the shape, but both motors are considered while in the transformation mode. Propulsive efficiency in the transformation mode is defined by the total power output and mechanical transmission power from the two motors, as shown below:

$$\eta = \frac{P_u}{P_w} = \frac{P_u}{(P_{a1} - P_{m1}) + (P_{a2} - P_{m2})}, \tag{7}$$

where $P_{a1}$ and $P_{a2}$ denote the total output power of the oscillating motor and the transformation motor, respectively, $P_{m1}$ and $P_{m2}$ denote the mechanical transmission power of the oscillating motor and the transformation motor, respectively.

## 3. Experimental results and analysis

The transformable robotic fin and dragging experimental platform enable us to explore the propulsive performance of the robotic fin in various kinematic parameters and controlling modes.

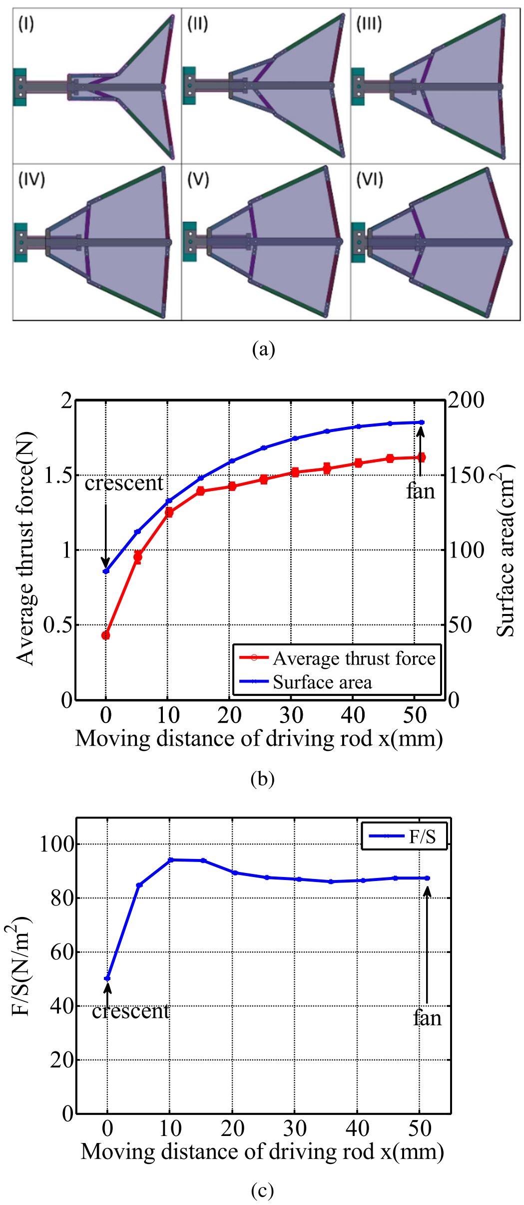


**Figure 5.** Effect of transforming the fin with $f = 1$ Hz, $\theta = 30°$ and $v = 0.25\ L$. (a) Several intervening states from crescent to fan with different moving distance of driving rod $x$: (I) $x = 0$ mm, (II) $x = 10.24$ mm, (III) $x = 20.48$ mm, (IV) $x = 30.72$ mm, (V) $x = 40.96$ mm, (VI) $x = 51.2$ mm. (b) The dynamics of surface area and average thrust force, along with the moving of the driving rod. (c) The dynamics of thrust force per unit area along with movement of the driving rod.

### 3.1. Influence of surface areas

The robotic fin can be transformed from a crescent to a fan smoothly, during which time its surface area also changes. We first examined how variable surface areas affected propulsion during a steady swimming state. Figure 5(a) shows the robotic fin in various stages of transformation where propulsive performance was studied in a steady state. Figures 5(b) and (c) present the average thrust force and average thrust force per unit area of the fin with respect to displacement of the driving rod, respectively. Here, $x$ denotes the distance the driving rod moved while being pulled by the non-elastic cable, while $F/S$ denotes the average thrust force per unit area of the fin.

Figure 5 also shows how the fin was transformed from crescent to fan as the driving rod moved from 0 to 51.2 mm. During this process the surface area of the robotic fin increased more than twice its original size. Figure 5(b) shows, during the process of transformation, the surface area and average thrust force increased almost synchronously. The thrust force per unit area is extracted to describe the influence of surface area defined by $F/S$, as shown in figure 5(c). Note that when $x$ is equal to 10.24 mm, the thrust force per unit area is at its maximum, but when the driving rod moved from 30.72 to 51.2 mm, there was only a small deformation and the thrust force per unit area remained stable.

Although *F/S* of the moment $x$ at 10.24 mm was the maximum value, we still changed the shape from crescent to fan to analyze the locomotion performance according to the study of Webb [21].

**Table 2.** Parameters used in three groups of experiments.

| Parameter | Specific value |
|---|---|
| Change frequency | |
| Oscillating frequency | 0.25 Hz 0.5 Hz 1 Hz |
| Oscillating amplitude | 30° |
| Drag velocity | 0.25 $L$ |
| Change amplitude | |
| Oscillating frequency | 1 Hz |
| Oscillating amplitude | 15° 20° 25° 30° |
| Drag velocity | 0.25 $L$ |
| Change drag velocity | |
| Oscillating frequency | 1 Hz |
| Oscillating amplitude | 30° |
| Drag velocity | $-0.5\ L$ $-0.25\ L$ 0 0.25 $L$ 0.5 $L$ |

### 3.2. Influence of kinematic parameters

Three groups of experiments were carried out to explore the influence of the kinematic parameters, with the control variable method being used to ensure that each experiment had a single variable value. The kinematic parameters used in the experiments are listed in table 2.

Figure 6 presents a comparison of the thrust force, the average thrust force, and the efficiency by experimental measurement. To obtain the condition for a single variable parameters, we varied the frequency, amplitude, and drag velocity, while keeping the other two parameters constant.

The results of varying frequencies are shown in figures 7(a) and (b). In the experiments, the oscillating amplitude and drag velocity of the fin were constant at 30° and 0.25 $L$/ s, which shows that the peaks and valleys of the thrust force trajectories increased as the frequency increased. Figure 6(b) shows that changes in

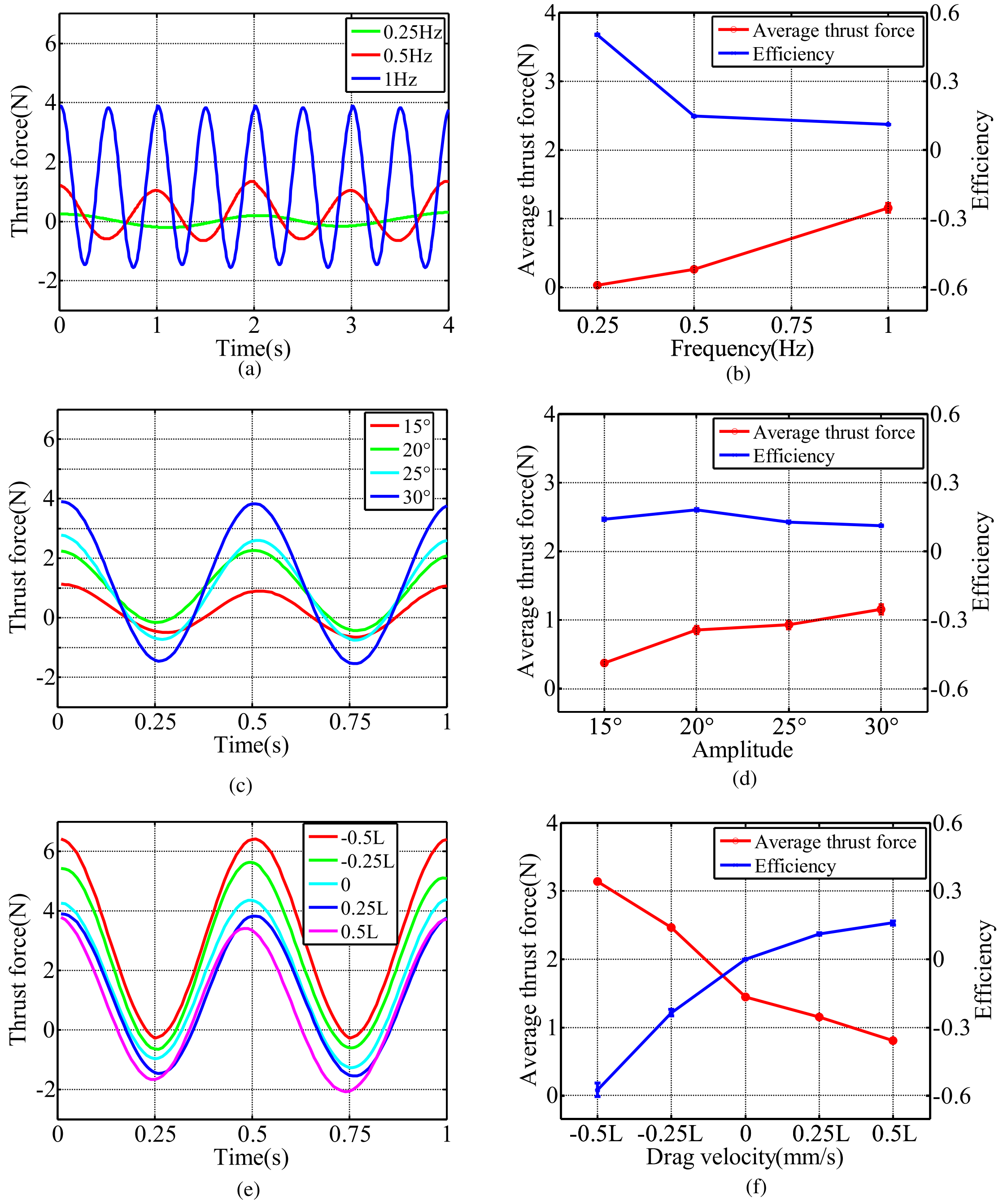


**Figure 6.** Comparison of thrust force, average thrust force and efficiency. (a) and (b) Thrust force, average thrust force and efficiency at variable frequency with $\theta = 30°$ and $v = 0.25\ L$. (c) and (d) Thrust force, average thrust force and efficiency at different amplitude with $f = 1$ Hz and $v = 0.25\ L$. (e) and (f) Thrust force, average thrust force and efficiency at different drag velocity with $f = 1$ Hz and $\theta = 30°$.

the average thrust force and its efficiency differed in that if the frequency increased, the average thrust force increased and efficiency decreased. The increasing of the oscillating frequency leads to a rapid oscillating of the fin and then a larger thrust force. However, the total output power consumption $P_a$ and mechanical energy consumption $P_m$ both increased during the increasing of the frequency. And the total consumption $P_w$ increased faster than the thrust force did, which leads to a lower propulsive efficiency.

Figures 7(c) and (d) shows the result of varying the oscillating amplitude. Here, the increasing of the oscillating amplitude also leads to the increasing of the average thrust force. Moreover, the change of the oscillating amplitude has smaller effect on the propulsive efficiency. Hence, the efficiency of different oscillating amplitude ranging from 15° to 30° kept stable.

The influence of the drag velocity is shown in figures 7(e) and (f). Here the average thrust force decreased as the drag velocity ranged from $-0.5\ L/\mathrm{s}$ to $0.5\ L/\mathrm{s}$, while the change in efficiency was opposite. The result also indicates that a higher propulsive efficiency and a higher thrust force cannot be achieved simultaneously.

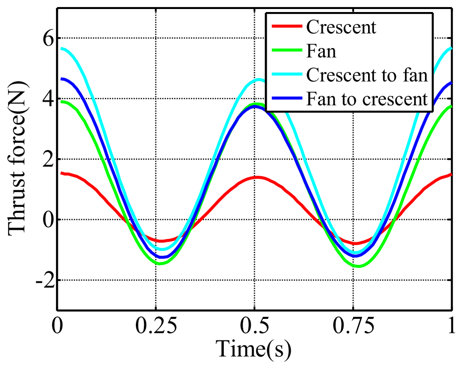


(a)

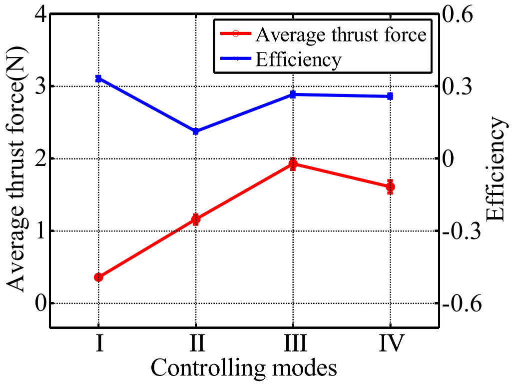


(b)

**Figure 7.** Thrust force, average thrust force and efficiency of variable controlling modes with $f = 1$ Hz, $\theta = 30°$ and $v = 0.25\ L$. (a) Thrust force in one cycle. (b) Average thrust force and efficiency with respective to controlling modes. I, II, III and IV denotes crescent mode, fan mode, crescent to fan mode, and fan to crescent mode, respectively.

It is noted from figures 7(a), (c) and (e) that all thrust force trajectories exhibit fine sine curves, which indicates that the interference from the wall of the water tank and the water surface cause a small effect to the thrust force. From figures 7(b), (d) and (f), it can be seen that the change of the average thrust force and the change of propulsive efficiency differs, which means it is hard to achieve a higher propulsive efficiency and a higher thrust force simultaneously just varying the kinematic parameters of the robotic fin. However, the result also indicates that the robotic fin can vary its kinematic parameters to achieve different performance to satisfy different requirements.

### 3.3. Influence of controlling modes

We also conducted a series of experiments with variable controlling modes and the same kinematics in order to investigate the influence of the controlling modes, and the results are shown in figure 7.

The thrust force of the fin with four controlling modes is shown in figure 7(a), and indicates that the maximum thrust force in crescent mode was almost completely different to the other modes. The thrust force of the fin from crescent to fan mode had the largest peak value and a slightly smaller valley value than the fin in crescent mode. That means the crescent to fan mode can reach maximum instantaneous thrust force, whereas the fan to crescent mode is similar to the crescent to fan mode. Two transformation modes can produce a larger thrust force that will help a robotic fish swim away from a complex environment.

Figure 7(b) shows that crescent mode was the most efficient and fan mode was the least efficient, however, the two transformation modes are still more efficient than the fan mode. Moreover, the transformation modes can produce much greater thrust forces than the two steady modes. Although the transformation modes require two motors, the efficiency is still higher than the steady state modes due to the higher average propulsive thrust. However, the two motors require more power for the transformation modes than the two steady modes, although different controlling modes can be selected according to the situation the robotic fish is in.

Comparing to the steady modes, the two transformation modes can generate higher thrust forces. Furthermore, the crescent to fan mode produced the largest thrust force. The reason for this phenomenon lies in that the fin changes shape to crescent during out-stroke stages (see figure 4), which leads to a small resistance. Moreover, it changes to fan during in-stroke stages (see figure 4), which leads to a larger thrust force. The average thrust force will then increase due to the transformation effect. It is worth to be noted that the average thrust force of fan to crescent mode is also larger than that of the fan mode. The phenomenon indicates that the transformation process alters the flow field to shed an positive impact on the average thrust force. It should be pointed out that the transformation modes can achieve a higher efficiency and a higher average thrust force simultaneously than adjusting the kinematic parameters do, which indicates the unique advantage of the transformable robotic fin.

## 4. Further analysis of the experimental results

In the previous section we examined how a single parameter and different controlling modes affects propulsion; here we will explore the propulsive performance of the fin with various kinematics in four controlling modes to determine the optimal way of improving the performance of a robotic fish in various environments or tasks.

### 4.1. Influence of oscillating amplitude and controlling modes

Figure 8 shows how the oscillating amplitude in four controlling modes performs when the frequency is 1 Hz and the drag velocity is 0.25 $L$/s. Figure 8(a)

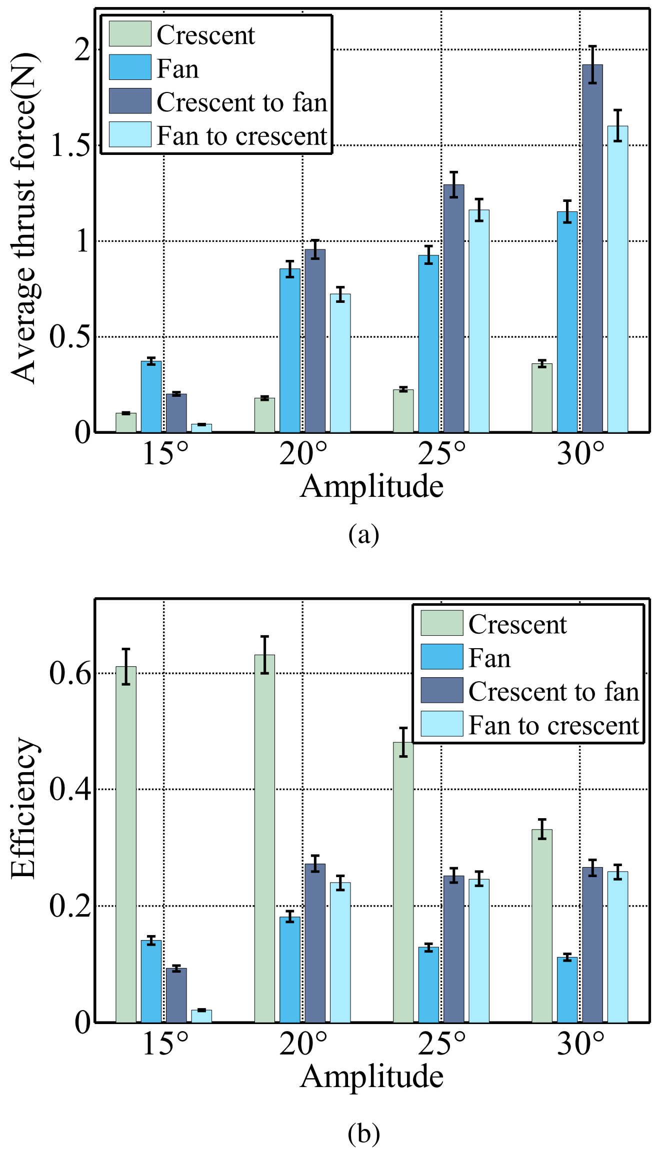


**Figure 8.** Effect of amplitude in four controlling modes with $f = 1$ Hz and $v = 0.25\ L$. (a) Average thrust force of different amplitude in four controlling modes. (b) Efficiency of different amplitude in four controlling modes.

shows that the average thrust force increases as the amplitude increases, while the average thrust force of the robotic fin in transformation modes has a higher value than in steady modes. The efficiency shown in figure 8(b) indicates that the crescent mode and fan mode are similar in that the propulsive efficiency increases when the oscillating amplitude is below 20° and decreases when the oscillating amplitude is above 20°. The efficiency of two transformation modes increases as the oscillating amplitude increases.

The crescent mode generates a smaller average thrust force for the least area of the robotic fin, However, it also consumed the least power so that its efficiency is the highest. Note that different controlling modes have different characteristics, so each controlling mode is suitable for a particular application. For example, the crescent to fan mode can be applied when the instantaneous acceleration at a large amplitude is needed to obtain the largest thrust force; the crescent mode is superior in power saving and has better performance for a long time cruising.

### 4.2. Influence of oscillating frequency and controlling modes

The oscillating frequency and controlling modes were investigated as shown in figure 9. Figure 9(a) shows that the average thrust force increased slightly in all controlling modes when the frequency increased from 0.25 to 0.5 Hz, but when the frequency increased from 0.5 to 1 Hz, the average thrust force increased sharply. Moreover, the fan mode generated the largest force when the frequency was 0.25 Hz or 0.5 Hz, whereas the crescent to fan mode had the largest thrust force when the frequency was 1 Hz.

It can be concluded from figure 9(b) that the two steady modes became less efficient as the frequency increased, but with the two transformation modes, the efficiency reached its lowest value when the frequency

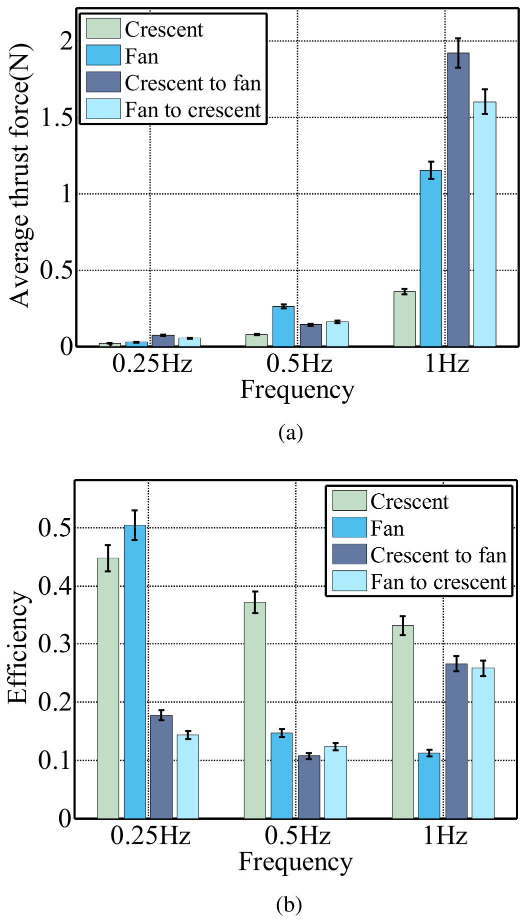


**Figure 9.** Influence of frequency in four controlling modes with $\theta = 30°$ and $v = 0.25\ L$. (a) Average thrust force of different frequency in four controlling modes. (b) Efficiency of different frequencies in four controlling modes.

was 0.5 Hz and the largest value when the frequency was 1 Hz. From the experimental result, it can be concluded that the transformable robotic fin could adopt better propulsive performance when the frequency is about 1 Hz. Note also that the transformation modes usually had better propulsion when the thrust force and efficiency were considered simultaneously, but the steady modes can also be applied when the frequency is low to help the robotic fish swim more effectively.

### 4.3. Influence of the drag velocity and controlling modes

Figure 10 shows how the drag velocity and controlling modes affect propulsion; figure 10(a) shows that the average thrust force in crescent mode, fan mode, and crescent to fan mode decreased from $-0.5\ L/\mathrm{s}$ to $0.5\ L/\mathrm{s}$, while the fan to crescent mode had a maximum value at 0 drag velocity.

Figure 10(b) shows that the efficiency of two steady modes were similar, while the two transformation modes became more efficient from $-0.5\ L/\mathrm{s}$ to $0.25\ L/\mathrm{s}$ and less efficient from $0.25\ L/\mathrm{s}$ to $0.5\ L/\mathrm{s}$.

The result of the experiment shows that the transformable robotic fin can achieve an optimal thrust force or efficiency by changing the controlling modes when encountering a changing environment with variable flow speed or a changing task.

## 5. Discussions

In one cyclic movement, a fish fin oscillates backwards and forwards to propel the fish forwards. Researchers have put forward several basic patterns in order to simplify these complex movements [46–48]. Unlike the shape of a single fin, a transformable robotic fin can adapt better to different environments and generate better propulsion. A novel transformable robotic fin has been developed where the shape can be changed by a driving motor, and so too can the surface area and aspect ratio.

This transformable fin can change from crescent to fan shape with various features; it can change shape while swimming to adapt to changing environments; it can also change shape in one oscillating cycle to improve propulsion. It is worth emphasizing that this robotic fin was not developed to fully replicate the morphology of a fin but to verify how to perform with an optimal way in various environment by changing shape of the fin during swimming.

The experimental result indicates that the transformation modes of the robotic fin can achieve higher propulsive performance, especially the crescent to fan mode and fan to crescent mode can generate higher thrust forces. However, the mechanism of the transformation propulsion still remains unknown, which needs the study of the hydrodynamics during transformation propulsion. The transformable fin performs transformation during oscillating, so the simulation of the process is quite difficult. Furthermore, the complex flow field caused by the shape change of the fin during oscillating is difficult to be measured experimentally. The hydrodynamic mechanism of transform modes of the robotic fin needs to be studied in the future.

The experimental results revealed that the dynamic change in the shape of the fin has a significant effect on how the surrounding fluid responds. However, one deformation mode did not always have the best effect for various kinematic parameters because as the amplitudes varied the crescent mode was the most efficient, and as the frequencies varied, the fan mode delivered the maximum average thrust force at 0.5 Hz. With the drag velocity, the fan to crescent mode had a maximum average thrust force at $0\ \mathrm{l\ s}^{-1}$ and a unique rule of efficiency, therefore different controlling modes must be applied at different kinematic parameters and environmental parameters to optimize swimming in full operating conditions for changing tasks.

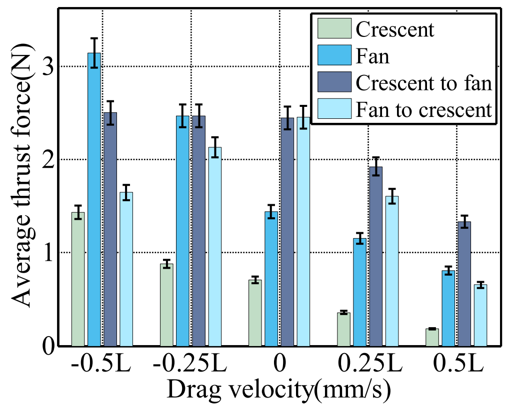


(a)

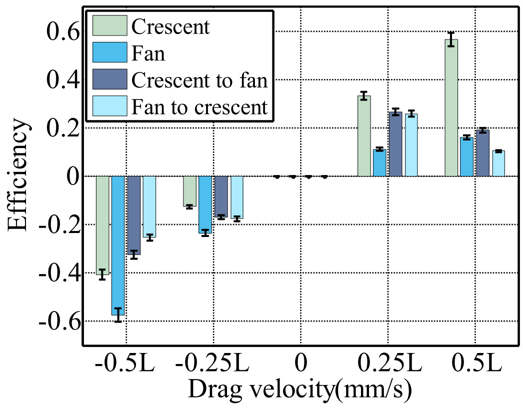


(b)

**Figure 10.** Influence of drag velocity in four controlling modes with $f = 1$ Hz and $\theta = 30°$. (a) Average thrust force of different drag velocity in four controlling modes. (b) Efficiency of different drag velocities in four controlling modes.

## 6. Conclusions

This paper proposes a novel transformable fish fin inspired by the ability of fish to change the shape of their fins while swimming. Although the frame of this fin is rigid, the skin is flexible. A multi-link mechanism driven by a motor was used to change the fin from crescent to fan while swimming. The surface area and aspect ratio of the fin also changes. Two motors were used to synchronize and realize the oscillating and shape changing motions. We investigated the characteristics of various fin shapes, and the influence he main kinematic parameters and controlling modes had on the thrust force and propulsive efficiency. We found that transformation modes in a cyclic motion can influence the hydrodynamic response in different ways. The oscillating kinematic parameters indicated that these parameters coupled with the controlling modes in a complicated way, but they did improve propulsion when the parameters were combined properly. These results delivered a comprehensive understanding of the complex deformation of the fin and its effect on the hydrodynamic forces, which can guide future designs of novel underwater robotic propulsive systems. Future work includes an accurate measurement of the flow field as the fin is transformed, in order to obtain an overall understanding of the propulsive performance of this transformable fin.

## Acknowledgments

This research is supported by National Natural Science Foundation of China (No. 51375468) and ARC Discovery Grant (DP150102636). The authors would like to thank Mr Yun Qian and Mr Dongqi Gao for their helpful discussions on setting up the experimental platform and conducting the experiments.

## References

[1] Lightill M J 1971 Large-amplitude elongated-body theory of fish locomotion *Proc. R. Soc.* B **179** 125–38
[2] Wu T Y 1971 Hydromechanics of swimming propulsion: I. Swimming of a two-dimensional flexible plate at variable forward speeds in an inviscid fluid *J. Fluid Mech.* **46** 337–55
[3] Triantafyllou M S and Triantafyllou G S 1995 An efficient swimming machine *Sci. Am.* **272** 64–70
[4] Park S J *et al* 2016 Phototactic guidance of a tissue-engineered soft-robotic ray *Science* **353** 158–62
[5] Lindsey C C 1978 Form, function and locomotory habits in fish *Fish Physiol.* **7** 1–100
[6] Sfakiotakis M, Lane D M and Davies J B C 1999 Review of fish swimming modes for aquatic locomotion *IEEE J. Ocean. Eng.* **24** 237–52
[7] Westneat M, Thorsen D H, Walker J A and Hale M 2004 Structure, function, and neural control of pectoral fins in fishes *IEEE J. Ocean. Eng.* **29** 674–83
[8] Thorsen D H and Westneat M W 2005 Diversity of pectoral fin structure and function in fishes with labriform propulsion *J. Morphol.* **263** 133–50
[9] Webb P W 2006 Stability and maneuverability *Fish Biol.* **23** 281–332
[10] Rosenberger L J and Westneat M W 1999 Functional morphology of undulatory pectoral fin locomotion in the stingray taeniura lymma (chondrichthyes: dasyatidae) *J. Exp. Biol.* **202** 3523–39
[11] Rosenberger L J 2001 Pectoral fin locomotion in batoid fishes: undulation versus oscillation *J. Exp. Biol.* **204** 379–94
[12] Wang L, Xu M, Liu B, Zhang S W and Yang J 2013 Experimental study on morphology and kinematics of mudskipper in amphibious environments *Proc. IEEE Int. Conf. on Robotics and Biomimetics* pp 1095–100
[13] Yang S B, Qiu J and Han X Y 2009 Kinematics modeling and experiments of pectoral oscillation propulsion robotic fish *J. Bionic. Eng.* **6** 174–9
[14] Low K H 2009 Modeling and parametric study of modular undulating fin rays for fish robots *Mech. Mach. Theory* **44** 615–32
[15] Yan Q, Wang L, Liu B, Yang J and Zhang S W 2012 A novel implementation of a flexible robotic fin actuated by shape memory alloy *J. Bionic Eng.* **9** 156–65
[16] Zhang S W, Liu B, Yan Q, Wang L, Low K H and Yang J 2014 Design and implementation of a lightweight bio-Inspired pectoral fin with complex motions *IEEE/ASME Trans. Mech.* **19** 1773–85
[17] Liu B, Zhang S W, Qin F H and Yang J 2014 Fluid-structure interaction study on the performance of flexible articulated caudal fin *Adv. Robot.* **28** 1665–76
[18] Lauder G V, Madden P G A, Mittal R, Dong H and Bozkurttas M 2006 Locomotion with flexible propulsors: I. Experimental analysis of pectoral fin swimming in sunfish *Bioinsp. Biomim.* **1** s25–34

[19] Lauder G V, Anderson E J, Tangorra J L and Madden P G A 2007 Fish biorobotics: kinematics and hydrodynamics of self-propulsion *J. Exp. Biol.* **210** 2767–80

[20] Flammang B E and Lauder G V 2009 Caudal fin shape modulation and control during acceleration, braking and backing maneuvers in bluegill sunfish lepomis macrochirus *J. Exp. Biol.* **212** 277–86

[21] Webb P W 1984 Form and function in fish swimming *Sci. Am.* **251** 72–82

[22] Yan Q, Han Z, Zhang S W and Yang J 2008 Parametric research of experiments on a carangiform robotic fish *J. Bionic. Eng.* **5** 95–101

[23] Liu J D and Hu H S 2010 Biological inspiration: from carangiform fish to multi-joint robotic fish *J. Bionic. Eng.* **7** 35–48

[24] Wen L, Wang T M, Wu G H and Liang J H 2012 Hydrodynamic investigation of a self-propelled robotic fish based on a force-feedback control method *Bioinsp. Biomim.* **7** 036012

[25] Yu J, Liu L, Wang L, Tan M and Xu D 2008 Turning control of a multilink biomimetic robotic fish *IEEE Trans. Robot.* **24** 201–6

[26] Clapham R J and Hu H S 2014 iSplash-II: Realizing fast carangiform swimming to outperform a real fish *IEEE/RSJ Int. Conf. on Intelligent Robots and Systems (Germany/Austria)* pp 1080–6

[27] Chen Z, Shatara S and Tan X B 2010 Modeling of biomimetic robotic fish propelled by an ionic polymer–metal composite caudal fin *IEEE/ASME Trans. Mech.* **15** 448–59

[28] Wu Z X, Yu J Z, Tan M and Zhang J W 2014 Kinematic comparison of forward and backward swimming and maneuvering in a self-propelled sub-carangiform robotic fish *J. Bionic Eng.* **11** 199–212

[29] Wang J X and Tan X B 2013 A dynamic model for tail-actuated robotic fish with drag coefficient adaptation *Mechatronics* **23** 659–68

[30] Chong C W, Zhong Y, Zhou C L, Low K H and Seet G 2009 Can the swimming thrust of BCF biomimetics fish be enhanced? *Proc. IEEE Int. Conf. on Robotics and Biomimetics (Bangkok, Thailand)* pp 437–42

[31] Yamamoto I, Terada Y, Nagamatu T and Imaizumi Y 1995 Propulsion system with flexible rigid oscillating fin *IEEE J. Ocean. Eng.* **20** 23–30

[32] Heathcote S, Martin D and Gursul I 2004 Flexible flapping airfoil propulsion at zero freestream velocity *AIAA J.* **42** 2196–204

[33] Low K H and Chong C W 2010 Parametric study of the swimming performance of a fish robot propelled by a flexible caudal fin *Bioinsp. Biomim.* **5** 046002

[34] Lucas K N, Thornycroft P J M, Gemmell B J, Colin S P, Costello J H and Lauder G V 2015 Effects of non-uniform stiffness on the swimming performance of a passively-flexing, fish-like foil model *Bioinsp. Biomim.* **10** 056019

[35] Anton M, Chen Z, Kruusmaa M and Tan X B 2009 Analytical and computational modeling of robotic fish propelled by soft actuation material-based active joints *IEEE-RSJ Int. Conf. on Intelligent Robots and Systems* pp 2126–31

[36] Liu B, Yang Y K, Qin F H and Zhang S W 2015 Performance study on a novel variable area robotic fin *Mechatronics* **32** 59–66

[37] Neveln I D, Bale R, Bhalla A P S, Curet O M, Patankar N A and MacIver M A 2014 Undulating fins produce off-axis thrust and flow structures *J. Exp. Biol.* **217** 201–13

[38] Tangorra J L, Davidson S N, Hunter I W, Madden P G A, Lauder G V, Dong H, Bozkurttas M and Mittal R 2007 The development of a biologically inspired propulsor for unmanned underwater vehicles *IEEE J. Ocean. Eng.* **32** 533–50

[39] Tangorra J L, Lauder G V, Hunter I W, Mittal R, Madden P and Bozkurttas M 2010 The effect of fin ray flexural rigidity on the propulsive forces generated by a biorobotic fish pectoral fin *J. Exp. Biol.* **213** 4043–54

[40] Hu T, Shen L, Lin L and Xu H 2009 Biological inspirations, kinematics modeling, mechanism design and experiments on an undulating robotic fin inspired by Gymnarchus niloticus *Mech. Mach. Theory* **44** 633–45

[41] Nevelnb I D, Rothc E, Mitchelld T, Snyderb J, MacIverb M, Fortuneg E and Cowana N 2013 Mutually opposing forces during locomotion can eliminate the tradeoff between maneuverability and stability shahin sefatia *Proc. Natl Acad. Sci.* **110** 18798–803

[42] Neveln I D, Bai Y, Snyder J B, Solberg J R, Curet O M, Lynch K M and MacIver M A 2013 Biomimetic and bio-inspired robotics in electric fish research *J. Exp. Biol.* **216** 2501–14

[43] MacIver M A, Fontaine E and Burdick J W 2004 Designing future underwater vehicles: principles and mechanisms of the weakly electric fish *IEEE J. Ocean. Eng.* **29** 651–9

[44] Lauder G V and Tytell E D 2005 Hydrodynamics of undulatory propulsion *Fish Physiol.* 23 425–68

[45] Wernli R L 1999 AUVs—the maturity of the technology *MTS/IEEE OCEANS'99 (Seattle, WA)* pp 189–95

[46] Ruiz-Torres R, Curet O M, Lauder G V and MacIver M A 2014 Kinematics of the ribbon fin in hovering and swimming of the electric ghost knifefish *J. Exp. Biol.* **216** 823–8

[47] Bozkurttas M, Mittal R, Dong H, Lauder G V and Madden G A 2009 Low-dimensional models and performance scaling of a highly deformable fish pectoral fin *J. Fluid Mech.* **631** 311–42

[48] Wang L, Xu M, Liu B, Low K H, Yang J and Zhang S W 2013 Three-Dimensional kinematics analysis of the Koi Carp pectoral fin by digital image processing *J. Bionic Eng.* **10** 210–21